Invited Talk for the International Meeting on Storage Ring Physics, Flaine, France, February 22 - 28, 1975

LBL-4817
c. 1

NEW STATES IN THE DECAYS OF ψ(3095) AND ψ(3684)

J. S. Whitaker

March 1976

Prepared for the U. S. Energy Research and Development Administration under Contract W-7405-ENG-48

0 0 0 0 4 5 0 2 0 0 6

LBL-4817

NEW STATES IN THE DECAYS OF $\psi(3095)$ AND $\psi(3684)$

J. S. WHITAKER
Lawrence Berkeley Laboratory
University of California
Berkeley, California 94720 (USA)

Abstract: Preliminary analysis of new data on radiative decays of $\psi(3095)$ and $\psi(3684)$ confirms the existence of $\chi(3410)$ and of further structure in the 3.45 - 3.60 GeV region. The monochromatic photon from the transition $\psi(3684) \rightarrow \gamma\chi(3410)$ is observed in the inclusive photon spectrum from $\psi(3684)$; the branching ratio for this decay is $7 \pm 3\%$. We see no evidence for a state near 2.8 GeV reached in $\psi(3095)$ decays.

Résumé: Une analyse preliminaire de nos nouveaux résultats concernant les désintegrations radiatives du $\psi(3095)$ et $\psi(3684)$ confirme l'existence du $\chi(3410)$ et la presence de structure additionelle dans la region 3.45 - 3.60 GeV. Le photon monochromatique produit par la transition $\psi(3684) \rightarrow \gamma\chi(3410)$ est observé dans le spectre des photons du $\psi(3684)$; le rapport de branchement pour cette désintegration est $7 \pm 3\%$. Nous n'avons aucune indication d'un état près de 2.8 GeV provenant de désintegrations du $\psi(3095)$.

I. INTRODUCTION

We report here the results of preliminary analysis of new data on radiative decays of $\psi(3095)$ and $\psi(3684)$ (ψ and ψ') observed with the SLAC-LBL magnetic detector at SPEAR.[1] We now have $\sim$ 150,000 ψ events and $\sim$ 350,000 ψ' events, although not all the analysis is based on the full data sample. The analysis has followed three courses:

(1) detection of new states through their decays to all-charged particles,

(2) study of the inclusive photon spectra from ψ and ψ',

(3) study of ($\psi\gamma$) masses in $\psi' \to \gamma\gamma\psi$ decays.

Similar analyses as (1) and (3) on a smaller data sample have been published previously.[2,3]

II. CHARGED-PARTICLE DECAYS OF NEW STATES

In the first method, we use missing mass information to select events consistent with the hypothesis of a radiative decay from ψ or ψ' to some state X which then decays to only charged particles, all of which are identified in the detector. Events are first required to have all prongs originating in the interaction region, and the total charge must be zero. To eliminate $\psi' \to \pi^+\pi^-\psi$ events, an event is rejected if the missing mass against a $\pi^+\pi^-$ pair lies in the range 3.0 - 3.4 GeV. The missing mass against all the observed particles is then calculated assuming a mass assignment for the detected particles which must be consistent with the measured masses of those particles for which the measurement was possible. The missing mass is required to be consistent with zero within its error. Events passing these cuts are constrained to fit the selected channel plus a missing photon. There is no ambiguity in the channel assignment except between the $\pi^+\pi^-$ and K^+K^- channels, since for channels with four or more particles an incorrect mass assignment will move the missing mass away from zero and outside the cut.

Figure 1a shows the mass of the charged particles for events fitting $\psi' \to \gamma + 4\pi^{\pm}$. There is a clear peak at $\sim$ 3.41 GeV, with a width consistent with the expected resolution. In the region 3.45 - 3.60 GeV there is more structure which is broader than the resolution and is inconsistent with being a single narrow state. The hatched region in this and subsequent figures marks events which fit the decay channel with zero missing mass.

Figure 1b shows the mass spectrum from a similar analysis at the ψ. There are no significant bumps other than the elastic peak, the rest of the spectrum having the shape expected from $\psi \rightarrow \pi^+\pi^-\pi^+\pi^-\pi^o$.

Figure 2 shows the mass spectrum for events fitting $\psi' \rightarrow \gamma\pi^+\pi^-$ or γK^+K^-. The detector resolution is insufficient to choose between these channels; the hypothesis giving the smallest missing mass is divided approximately evenly between the two choices. Muons and electrons have been eliminated by range and pulse height criteria; the absence of elastic $\mu^+\mu^-$ or e^+e^- events indicates the leptonic background is negligible.

Figures 3 and 4 show the mass spectra for $\psi' \rightarrow \gamma\pi^+\pi^-K^+K^-$ and $\psi' \rightarrow \gamma\pi^+\pi^-p\bar{p}$ respectively. At this preliminary stage of the analysis we can conclude only that there is a consistent signal in the 3.41 GeV region and that with our present resolution and statistics we are unable to resolve the structure in the 3.45 - 3.60 GeV region. None of these channels from the ψ show any significant structure.

In Figs. 5a and 5b are shown the mass spectra for $\psi' \rightarrow \gamma 3(\pi^+\pi^-)$ with and without the cut against the cascade decay $\psi' \rightarrow \pi^+\pi^-\psi$. The clear signals in the 3.41 and 3.45 - 3.60 GeV regions are considerably affected by the cascade cut, complicating determination of the branching ratios.

The branching ratio product $B_f = \frac{\psi' \rightarrow \gamma X,\ X \rightarrow f}{\psi' \rightarrow \text{all}}$ is 0.1 - 0.2% for $X(3410)$ and for $X(3450-3600)$ and for each of the final states $2(\pi^+\pi^-)$, $\pi^+\pi^-K^+K^-$, and $3(\pi^+\pi^-)$. For $\psi' \rightarrow \gamma X(3410)$, $X(3410) \rightarrow \pi^+\pi^-$ or K^+K^- we now find $B_{\pi^+\pi^-/K^+K^-} = 6.5 \pm 1.8 \times 10^{-4}$, which is a factor of two smaller than the value reported at the 1975 Lepton-Photon Conference. In the $\psi' \rightarrow \gamma\pi^+\pi^-/K^+K^-$ channel there are four events at 3.54 ± 0.02 GeV; from these we calculate a 90% confidence upper limit of 2×10^{-4} for $[\psi' \rightarrow \gamma X(3450-3600),\ X \rightarrow \pi^+\pi^-/K^+K^-]/\psi' \rightarrow \text{all}$. From the data shown in

Fig. 1b we calculate an upper limit of 5×10^{-3} for $[\psi \to \gamma X(\sim 2800),\ X \to 4\pi^{\pm}]/\psi \to$ all.

III. INCLUSIVE PHOTON SPECTRA

Our second and third methods use the magnetic detector as a pair spectrometer, detecting the electron and positron from photon conversions in the material near the beam. The location and thickness of the effective converter are shown in Fig. 6; the total of 0.0515 radiation lengths gives a conversion probability for normally incident photons of 0.030 at 0.15 GeV and 0.039 at 2 GeV. The conversion products are detected by two proportional chambers followed by four double-gap spark chambers which cover the full azimuth and the polar angle from 45° to 135°. Particles from near the interaction region must have transverse momentum > 0.055 GeV/c to pass through enough chambers to be detected.

Photon conversions are recognized as pairs of oppositely charged particles with small invariant mass (assuming electron masses for the prongs). There is a complication due to the distributed radius of the effective converter, since the calculated pair mass depends on the assumed position of conversion. Requiring the mass of the pair to be less than 0.0275 GeV retains all the photon conversions and admits $\sim 20\%$ accidental background (estimated from like-charge pairs). Figure 7 shows the calculated detection probability for photons as a function of energy; conversion probability, polar angle acceptance, and the transverse momentum requirement are included. An isotropic photon distribution is assumed; if the photons are distributed as $1+\cos^2\theta$ the detection efficiency drops by $\sim 20\%$.

The photon energy is calculated as the scalar sum of the energies of the two charged particles. A number of effects contribute to the photon energy resolution, including charged particle momentum resolution and energy loss by the e^+ or e^- by ionization or radiation after conversion; the photon energy resolution varies from $\sim 2\%$ at 0.15 GeV to $\sim 5\%$ at 2 GeV.

The inclusive photon spectra for ψ and ψ' are plotted in Figs. 8 and 9. The ψ spectrum is reasonably smooth and shows the shape expected from the

π^o-generated continuum folded with the acceptance. The ψ' spectrum shows a $> 5\sigma$ peak at ~ 260 MeV, with the width expected from resolution. The peak remains at the same energy and width if the acceptance is decreased by a factor of two by increasing the charged particle transverse momentum requirement, indicating the peak is not being shaped by the acceptance. After correcting for mean energy loss by ionization the peak is at 263 ± 5 MeV; we identify this as the photon line due to $\psi' \rightarrow \gamma X(3410)$ which would have a 264 ± 10 MeV photon. The branching ratio for $\psi' \rightarrow \gamma X(3410)$ is calculated as

$$\frac{\Gamma[\psi' \rightarrow \gamma X(3410)]}{\Gamma(\psi')} = \frac{(\text{no. in peak})/\text{acceptance}/\text{RC}/\epsilon_{tr}^{s}}{(\text{no. total})/\epsilon_{tr}^{all}} ,$$

where ϵ_{tr}^{s} is the trigger efficiency when there is a ~ 260 MeV photon conversion inside the detector, ϵ_{tr}^{all} is the average trigger efficiency for all ψ' events, and RC is a correction for the possibility that the electron or the positron radiate enough energy to move the measured photon energy out of the peak. RC is calculated to be ~ 0.8; the ratio $\epsilon_{tr}^{all}/\epsilon_{tr}^{s}$ is determined by scanning for events in which the converted photon was essential to trigger and has the value 0.8 ± 0.2. The branching ratio for $\psi' \rightarrow \gamma X(3410)$ is $7 \pm 3\%$, assuming isotropic production of the photon, and $8.5 \pm 4\%$ for $1 + \cos^2\theta$ distribution. The error is dominated by systematics; the statistical error alone is $\pm 1.4\%$.

The absence of a peak in the ψ spectrum around 280 MeV indicates the rate for transitions from ψ to a state around 2.8 GeV is small; assuming reasonable hadronic decays of such an object we calculate a conservative upper limit of 10% for $\psi \rightarrow \gamma X(\sim 2.8)$. However, if the mass of X is much above 2.85 the photon line will fall in a region of small and rapidly varying acceptance and this limit would not apply. More detailed analysis will be necessary to address the question of possible additional structure in the ψ and ψ' photon spectra.

IV. $\psi' \rightarrow \gamma\gamma\psi$

Photon conversions allow us to identify events $\psi' \rightarrow \gamma\gamma\psi$, where one of the photons converts and the ψ is detected by its $\mu^+\mu^-$ decay. $\psi' \rightarrow \eta\psi$ events are eliminated by requiring the missing-mass-squared against the ψ to be less than 0.27 GeV^2; the small $\psi' \rightarrow \pi^0\pi^0\psi$ background is reduced by requiring the missing mass against the $e^+e^-, \mu^+\mu^-$ system to be consistent with zero. There is no background from $\psi' \rightarrow \pi^+\pi^-\psi$ since the $\pi^+\pi^-$ mass peaks strongly at large values.[4] Events passing these cuts are constrained to $\psi' \rightarrow \gamma\gamma\psi$. For each event there are two solutions for the $\psi\gamma$ mass; these are plotted against one another in Fig. 10. There is a clear accumulation at ~ 3.50 in the high mass projection (which is also favored by the absence in the ψ' inclusive photon spectrum of a line corresponding to the low mass solution). The few additional events outside this peak may indicate the presence of more states.

In summary, preliminary studies of new data on ψ and ψ' decays have verified the existence of the $\chi(3410)$ as a narrow state, with the rate $\psi' \rightarrow \gamma\chi(3.41)$ estimated to be $7 \pm 3\%$. The structure in the 3.45 - 3.60 GeV region persists, and we are as yet unable to resolve any substructure clearly. We do not see any evidence for a state near 2.8 GeV, either in its $4\pi^\pm$ decays or in the inclusive photon spectrum from the ψ.

This work was supported by the U. S. Energy Research and Development Administration.

REFERENCES

1. J.-E. Augustin et al., Phys. Rev. Letters 34, 233 (1975).
2. G. J. Feldman et al., Phys. Rev. Letters 35, 821 (1975).
3. W. Tanenbaum et al., Phys. Rev. Letters 35, 1323 (1975).
4. J. A. Kadyk et al., LBL Report No. LBL-3687 (1975).

FIGURE CAPTIONS

Fig. 1. (a) Invariant mass of the charged particles for events fitting $\psi' \rightarrow 4\pi^{\pm}$ with zero missing mass. The hatched region in this and subsequent plots marks events fitting zero missing momentum.

(b) Invariant mass for $\psi \rightarrow 4\pi^{\pm}$.

Fig. 2. Invariant mass for $\psi' \rightarrow \pi^+\pi^-$ or K^+K^-.

Fig. 3. Invariant mass for $\psi' \rightarrow \pi^+\pi^- K^+K^-$.

Fig. 4. Invariant mass for $\psi' \rightarrow \pi^+\pi^- p\bar{p}$.

Fig. 5a (b). Invariant mass for $\psi' \rightarrow 6\pi^{\pm}$ with (without) the cut against $\psi' \rightarrow \pi^+\pi^-\psi$.

Fig. 6. Effective converter for photon conversions, showing radius and thickness in radiation lengths for each component.

Fig. 7. Acceptance for photon conversions, including geometric cuts and transverse momentum cuts.

Fig. 8. The observed inclusive photon spectrum for ψ.

Fig. 9. The observed inclusive photon spectrum for ψ'.

Fig. 10. For $\psi' \rightarrow \gamma\gamma\psi$ events where one photon converts, this shows the higher $(\psi\gamma)$ mass solution plotted against the lower mass solution.

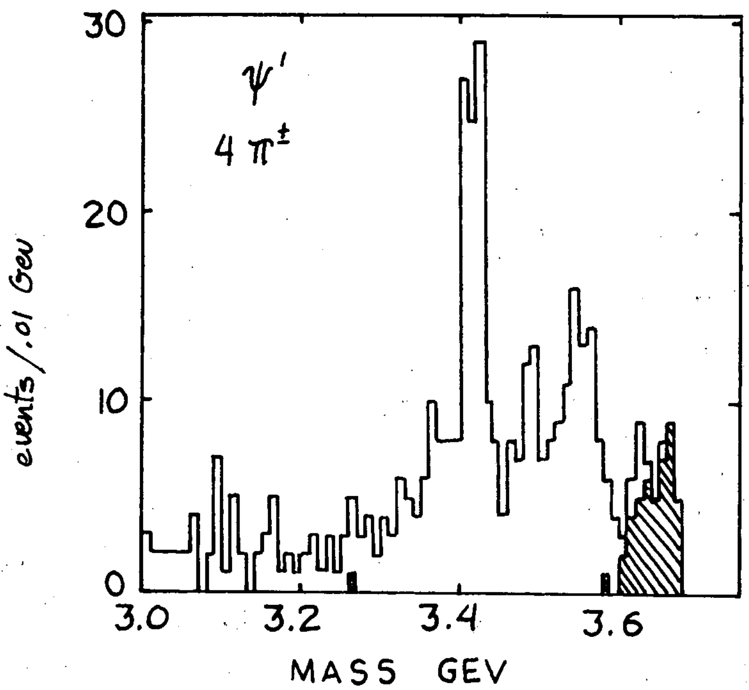

Fig. 1a

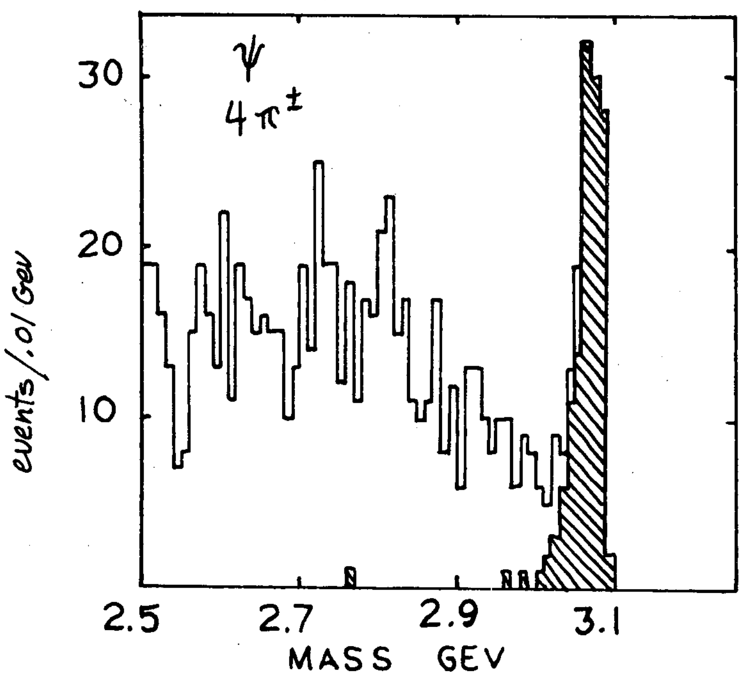

Fig. 1b

XBL 764-1106

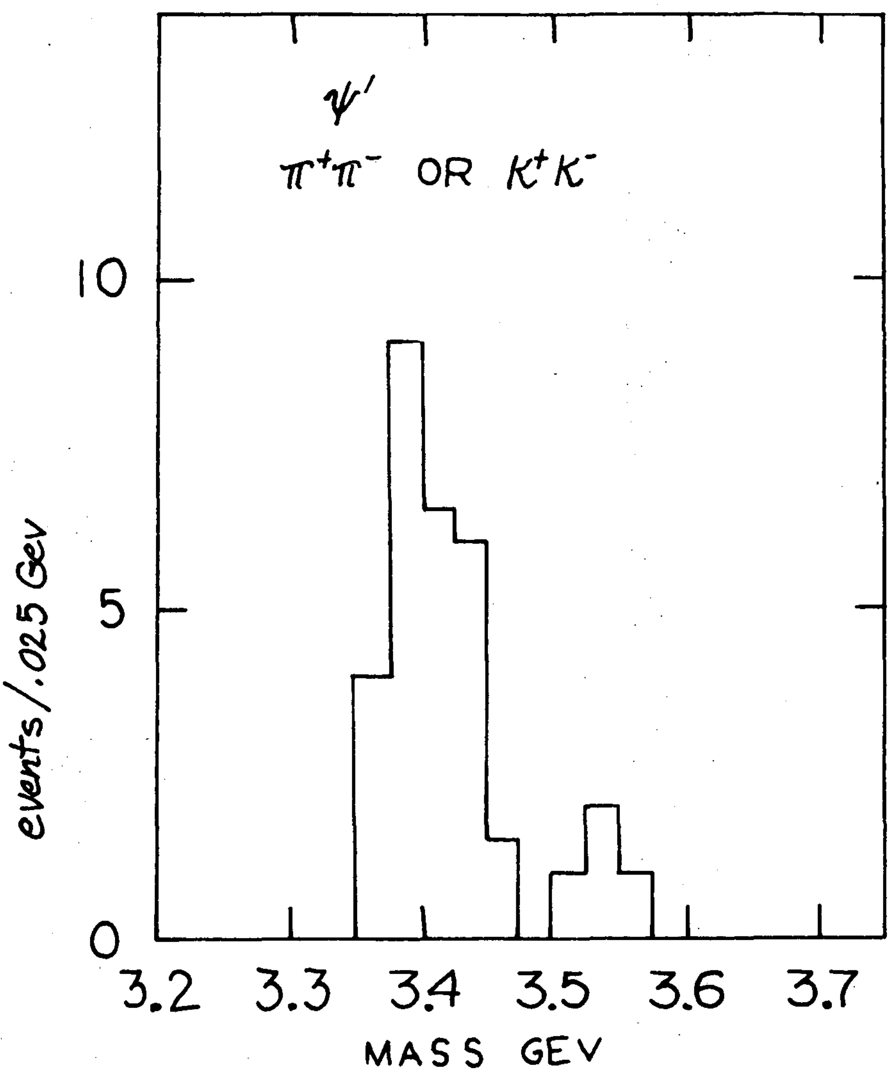

Fig. 2

XBL 764-1107

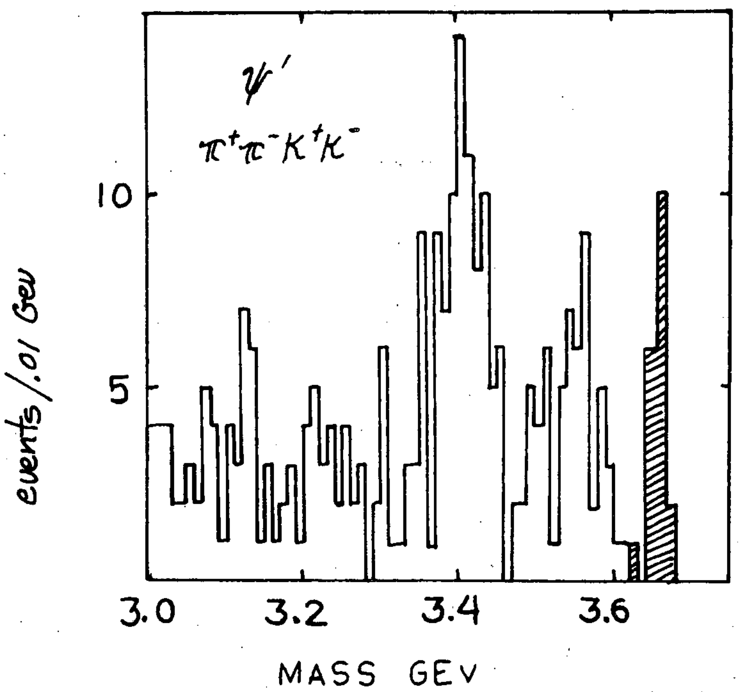

Fig. 3

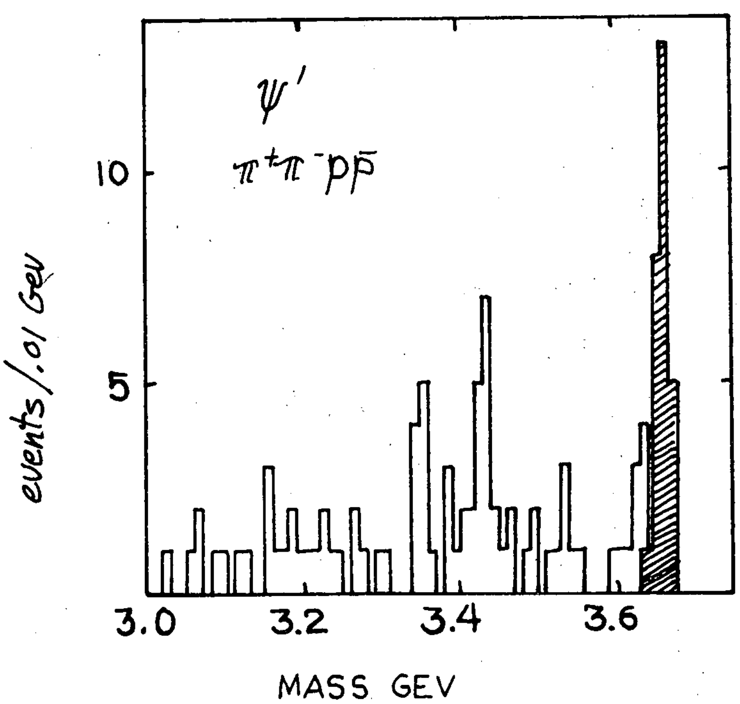

Fig. 4

XBL 764-1108

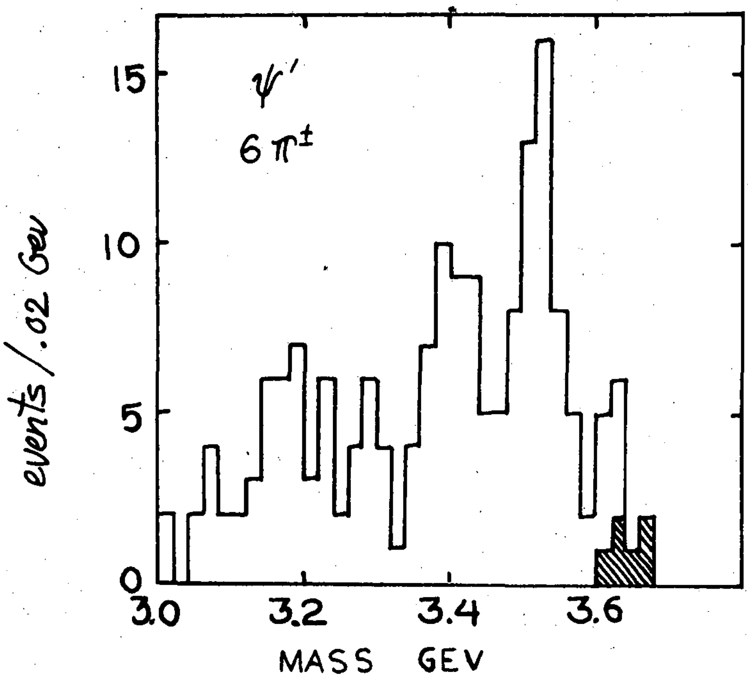

Fig. 5a

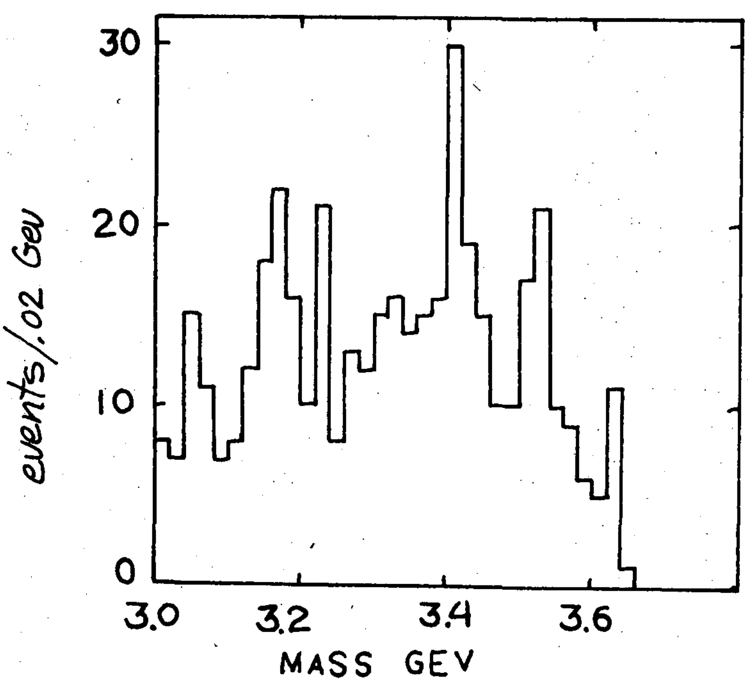

Fig. 5b

XBL 764-1109

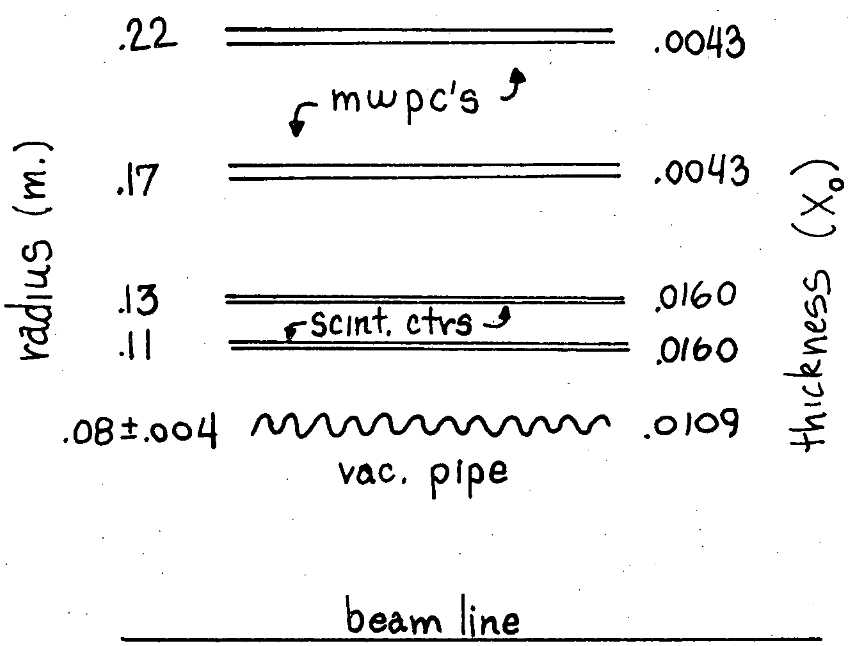

Fig. 6

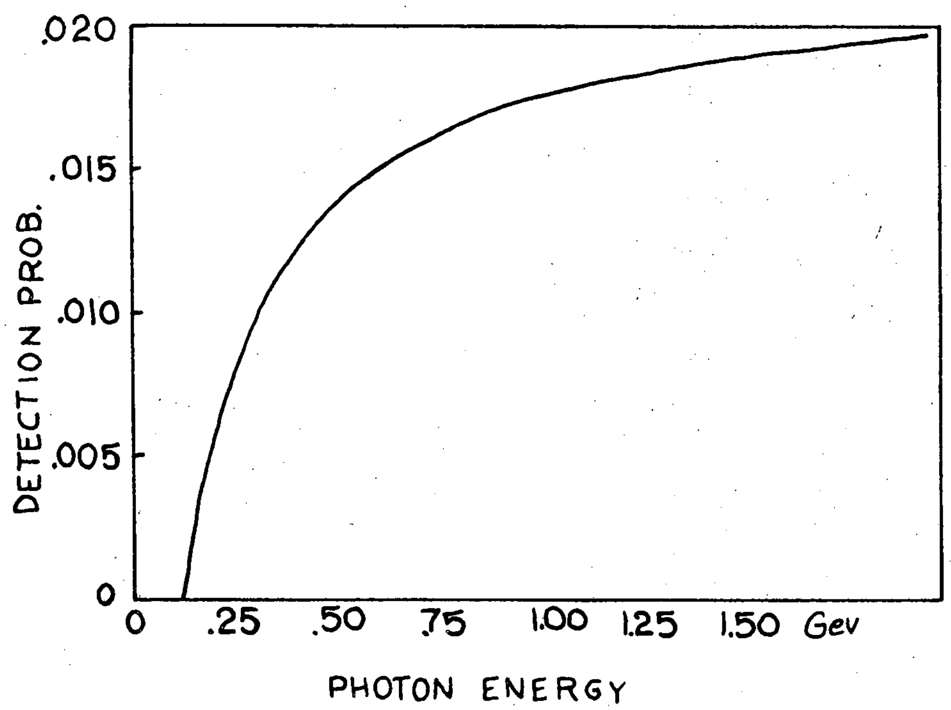

Fig. 7

XBL 764-1110

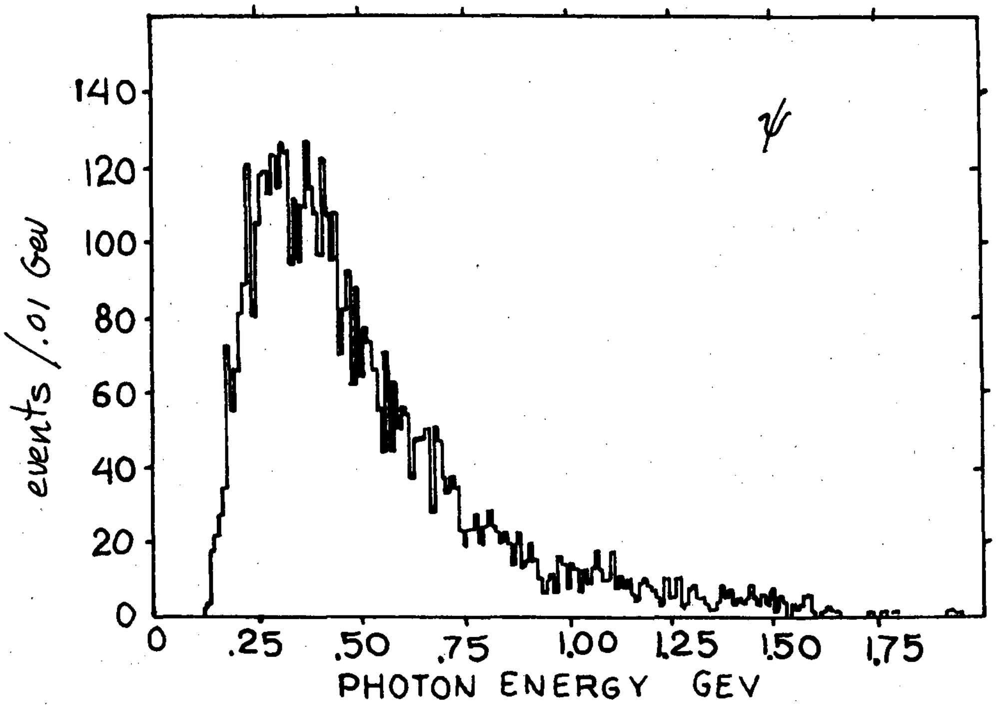

Fig. 8

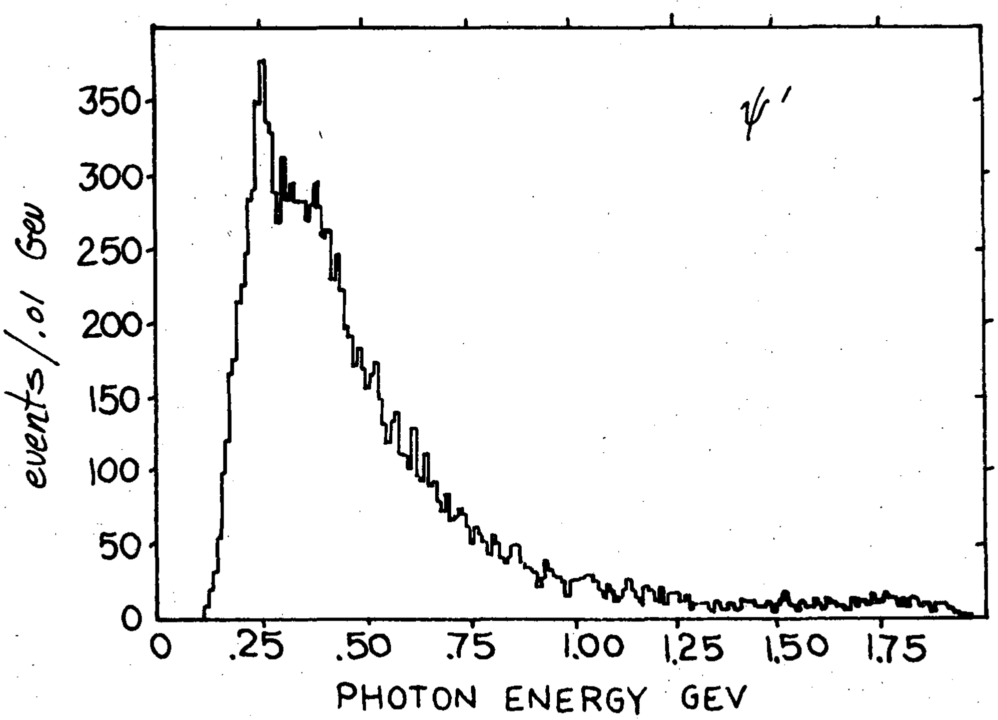

Fig. 9

XBL 764-1111

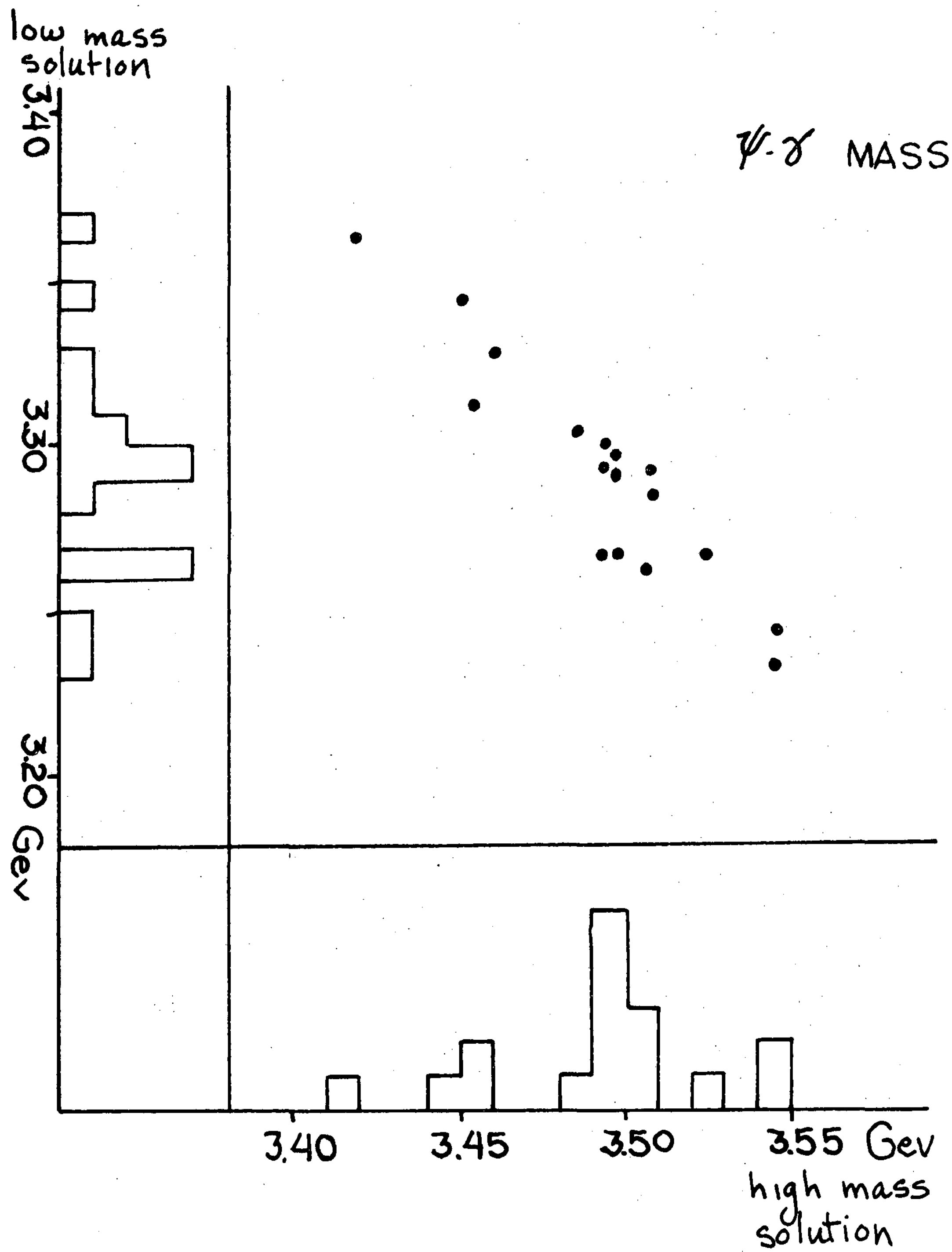

Fig. 10

XBL 764-1112